

Multimodal Rumor Detection Enhanced by External Evidence and Forgery Features

Han Li^{1,a} Hua Sun*

¹ *Information Engineering School of Dalian Ocean University
Dalian 116023, Liaoning, China*

^a*Email: lihanhenku20011115@163.com*

**Information Engineering School of Dalian Ocean University
Dalian 116023, Liaoning, China*

Email: sunhua@dlou.edu.cn

Abstract

Social media increasingly disseminates information through mixed image–text posts, but rumors often exploit subtle inconsistencies and forged content, making detection based solely on post content difficult. Deep semantic–mismatch rumors, which superficially align images and texts, pose particular challenges and threaten online public opinion. Existing multimodal rumor detection methods improve cross-modal modeling but suffer from limited feature extraction, noisy alignment, and inflexible fusion strategies, while ignoring external factual evidence necessary for verifying complex rumors. To address these limitations, we propose a multimodal rumor detection model enhanced with external evidence and forgery features. The model uses a ResNet34 visual encoder, a BERT text encoder, and a forgery-feature module extracting frequency-domain traces and compression artifacts via Fourier transformation. BLIP-generated image descriptions bridge image and text semantic spaces. A dual contrastive learning module computes contrastive losses between text–image and text–description pairs, improving detection of semantic inconsistencies. A gated adaptive feature-scaling fusion mechanism dynamically adjusts multimodal fusion and reduces redundancy. Experiments on Weibo and Twitter datasets demonstrate that our model outperforms mainstream baselines in macro accuracy, recall, and F1 score.

Keywords: Multimodal rumor detection; image–text semantic matching; modality fusion; attention mechanism; image forgery

1 Introduction

The rapid development of social networks enables various types of information to be widely disseminated within a very short period of time, which brings convenience to users while also providing favorable conditions for the generation and spread of false content. Driven by the traffic economy, online rumors have significantly improved in content breadth, dissemination speed, update frequency, and scope of influence, severely undermining online order and social trust. For example, in recent special rectification campaigns, relevant authorities have handled a large number of illegal accounts and rumor-related information according to law, highlighting the urgency of rumor governance in the social network environment. Meanwhile, with the diversification of communication forms, posts on social platforms are often accompanied by images, and rumor makers frequently combine real or synthetic images with false text, forming more deceptive image–text combinations [1]. Therefore, authenticity detection for multimodal posts on social networks, in order to achieve accurate rumor identification, has become a current research hotspot. Existing multimodal rumor detection models mostly crawl posts from social platforms, extract features of modalities such as text

and images, and fuse them to classify rumors. Although researchers have developed various models, several common issues remain. In the image-modality feature extraction stage, most studies focus on spatial-domain features [2] but ignore tampering traces in the frequency domain [3]. Although image-text consistency is often used as a judgment basis, the calculation of this consistency and its role in model decision-making are often unclear [4]. In terms of integrating social contextual features, due to the lack of explicit modeling of the post-comment-user interaction structure, models struggle to capture dissemination characteristics. Because structural noise widely exists in social network graphs, traditional graph neural networks easily learn misleading contextual features, affecting detection reliability. The feature extraction stage often relies on a single extraction method, resulting in insufficient mining of intra-modality heterogeneity. In the fusion stage, some methods only adopt simple concatenation and fail to handle semantic differences between modalities; although attention mechanisms are used, their usage methods and feature coverage remain limited [5]. To address the above challenges, this paper proposes a multimodal rumor detection framework that integrates forgery-feature extraction, dual contrastive learning module, and a gated fusion mechanism. In the visual branch, we design a forgery-feature extraction module based on Fourier transformation to capture potential image tampering traces. At the semantic level, we construct a dual contrastive mechanism that includes contrast between text and images as well as contrast between text and image descriptions, thereby reinforcing semantic alignment and suppressing the risk of noisy alignment. To address fluctuations in evidence quantity and modality noise, we design a gated modulation module that dynamically controls the multimodal feature fusion process through a learnable gating function combined with an adaptive feature-scaling mechanism, thereby improving control over modality flows and enhancing model robustness. Experimental results conducted on MR2 show that factors such as evidence quantity and forgery features significantly affect detection performance.

Overall, the main contributions of this paper include:

- (1) proposing a detection framework that integrates forgery features with cross-modal semantic features to address both semantic manipulation and visual-tampering attacks;
- (2) designing a gated fusion mechanism to achieve dynamic fusion of multimodal features and redundancy suppression;
- (3) Systematic experiments on multimodal rumor datasets demonstrate that the proposed method achieves an improvement in macro-accuracy compared to baseline methods.

2 Related Work

2.1 Monomodal Rumor Detection

Research on rumor and fake-news detection in social media has formed a multidimensional technical system, evolving from traditional machine learning relying on handcrafted features, to deep-learning sequence modeling, graph-structure mining, multimodal fusion, and finally to recent advances leveraging large language models (LLMs) and reinforcement learning. Existing monomodal rumor detection methods utilize features extracted from either text or images to detect rumors. Early rumor detection studies mainly focused on mining prominent features in the rumor propagation process and applied traditional machine-learning classifiers for identification. Kwon et al. [6] conducted an in-depth study on the temporal,

structural, and linguistic characteristics of rumor propagation, proposing a periodic external shock model to capture the cyclical outbreak features of rumors over time. They also found that isolated nodes have a higher proportion in rumor propagation networks, and that the frequency of negation words in rumor content is significantly higher than in non-rumor content. These studies provided important feature foundations for subsequent deep-learning models. To overcome the limitations of handcrafted features, researchers began using models such as recurrent neural networks (RNNs) to automatically learn high-dimensional features. Ma et al. [7] first applied RNNs to capture temporal variation features of tweet content. On this basis, Chen et al. [8] proposed the dARNN model, which employs a GRU with a deep attention mechanism (a variant of recurrent neural networks) to capture long-range dependencies in post sequences, thereby enabling the model to filter out highly discriminative key clues from the highly redundant early information. In addition, Alkhodair et al. [9] combined Word2Vec with LSTM to learn semantic features of text content, detecting sudden-news rumors related to emerging topics. Luvembe et al. [10] proposed a deep-normalization-based attention mechanism to extract dual emotional features of rumors. Moreover, to achieve near-real time source blocking, Xu et al. [11] proposed a topic-driven rumor detection framework (TDRD), which uses LDA to extract the topic distribution vector of the source microblog and combines it with content features extracted by a CNN. The study verifies that the importance and ambiguity of topics are key factors in the emergence of rumors, thereby enabling early near-real-time detection that relies solely on the source post without depending on subsequent interactions. With a lot of multimedia messages, text information often cannot prevent complex fraud. Cao et al. [12] mentioned in the literature that visual information helps detect fake news. They divide the visual features into foreground, semantic, statistical and contextual. Building on this view, Qi et al. [13] A multi-domain visual neural network (MVNN) was proposed. The network has several parts: extracting manipulation artifacts using a subnet of the frequency domain subnet, capture of semantic content with the branches of the pixel domain and a combination of the focus of text and multimodal classification, emphasize the complementarity of the frequency space and the representation of the pixel space. In addition to the visual modeling, rumor detection has also begun leveraging large language models (LLM). Huang et al. [14] offer FakeGPT, which is used to assess the effectiveness of ChatGPT in the generation, interpretation and detection of rumors, and also to include the causal consciousness. To eliminate the shortcomings of large models in the comprehensive verification of the facts of Zhang and Gao [15] offer the HiSS method. This method will destroy the claims that must be verified in small claims and then layered to verify them. This increases accuracy and leaves a clearer process of reasoning.

2.2 Multimodal Rumor Detection

With the evolution of the social media ecosystem, the forms of rumor propagation have shifted from single-text to multimodal formats that include images and videos, which has driven researchers to leverage cross-modal complementarity to enhance detection performance. Early work mainly focused on multimodal feature extraction and fusion. Wang et al. [16] offered EANN. EANN can study the expression of text and images using event discriminators to reduce bias, specificity for events, and improve the effect. Nguyen et al. [17] modeled inter-article dependencies with a deep Markov random field to support classification. Kirchknopf et al. [18] further extended multimodal inputs by incorporating user comments

and metadata via a multi-stream, hierarchical fusion design. Later-natured studies went beyond the “characteristic connection” and began to make obvious cross-modal interactions. Luembe et al. [19] introduced CAF-ODNN, using complementary attention to capture fine-grained text–image associations and attenuate irrelevant semantic noise. Liu et al. [20] proposed MVACNet, which promotes representation diversity through virtual augmented contrastive learning. Recently, the consistency-based approach as the main reference signal has become a semantic conflict of the image and text. Zhou et al. [21] quantified cross-modal mismatch via similarity modeling, while Xue et al. [22] developed a framework that explicitly explores multimodal consistency patterns for detection. On the basis of capturing the semantic consistency between text and images, the model further introduces the SRM filter to extract the physical statistical features of images, and significantly improves the capability of identifying high-quality forged images by detecting physical tampering traces such as synthesis and modification. Abdelnabi et al. [23] proposed the CCN network, which targets “out-of-context” fake news by retrieving external evidence from the open web and performing multi-dimensional consistency checking using features extracted by CLIP. However, Zhang et al. [24], through large-scale data analysis, challenged the traditional assumption that image–text inconsistency implies falsehood, pointing out that rumor makers often deliberately select highly matched images to increase deception, providing a new perspective for similarity-based detection methods. Although the above methods have achieved significant progress in feature mining and consistency detection, most rely solely on the content of the posts themselves and lack support from external knowledge, resulting in misjudgments when facing carefully fabricated rumors. So, now we are beginning to study the “evidence-based reasoning,” which is a new direction, but also the focus of this article. Wu et al. [25] two things were done: one was to create a Chinese multimodal rumor dataset called CSMRE, which contained evidence and the other to propose the EAMRD model. The model used a cross-attention mechanism to combine multimodal characteristics with the evidence found. To solve the problem that the model is subject to errors, Wu et al. [26] developed the ERD-DC model. The model uses a two-channel approach: on the one hand, it quickly finds old rumors of evidence, and discovers new rumors with multidimensional functions on the other, which can effectively balance the efficiency and accuracy. In addition, Huang et al. [27] offered the model DEETSA. This model combines a double improvement of evidence with the perception of the similarity of the image text, and also provides effective integration of multi-source information through adaptive gated networks.

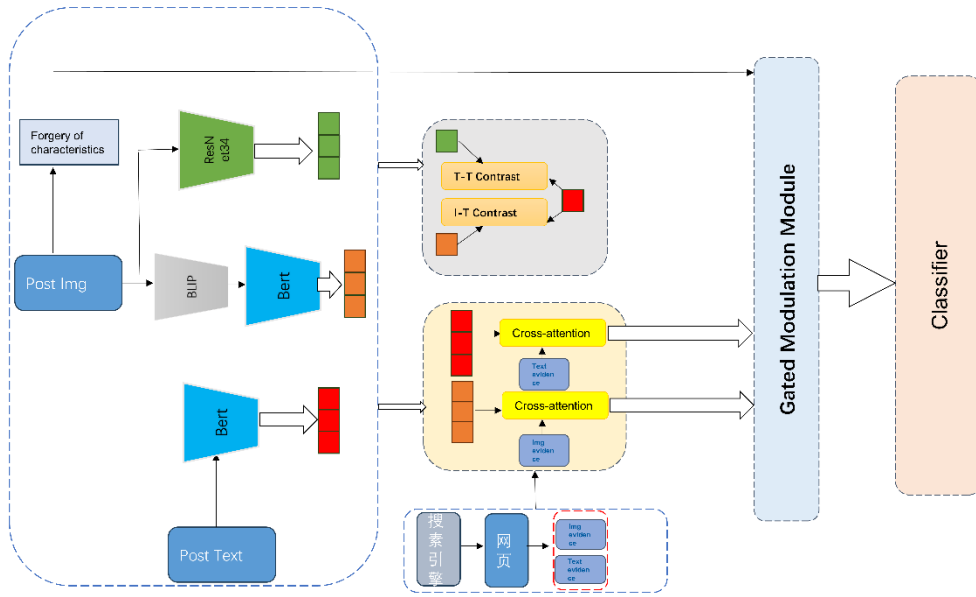


Figure 1. Model Structure Diagram

3 Methodology

This paper presents a multimodal rumor detection framework integrating external evidence and digital forgery features through the interaction of feature encoding, Dual contrastive learning module, evidence fusion, and gated modulation modules. This multi-layered architecture enables the exhaustive extraction and synthesis of salient features from complex multimodal streams to optimize detection performance, with the comprehensive structural mechanisms detailed in Figure 1.

3.1 Feature Extraction

In the multimodal rumor detection task, images and texts, as the two input modalities, differ not only in expression forms but also in information structure and semantic representation. To effectively extract meaningful features from these two modalities, the feature extraction module must be capable of deeply mining latent information in images and texts and mapping them into a unified feature space. This module combines image feature extraction, text feature encoding, and forgery-feature extraction, and enhances the alignment capability between images and texts through an effective fusion method.

3.1.1 Text Features

Text features are encoded using the BERT model. The BERT model, through a bidirectional Transformer encoder, is able to capture rich semantic information from context. After the textual data is input to BERT, the model learns representations of each word in context through its deep network. The goal of text feature encoding is to transform the original text into a high-dimensional semantic vector, which not only contains the specific meaning of words but also captures contextual relationships between words, thereby enabling learning of key information relevant to images, as follows:

$$h_T = \text{BERT}(T)$$

where T represents the input textual information, $h_T \in \mathbb{R}^{d_T}$ It represents the textual feature, and d_T denotes the dimensionality of this feature.

3.1.2 Image Features

Image features are encoded using the ResNet34 network. ResNet34 is a deep residual network that addresses the gradient vanishing problem in deep neural networks through residual blocks, allowing the network to handle deeper structures. This model is capable of extracting high-dimensional visual features from images and learning key information contained in them, as follows:

$$h_I = \text{ResNet34}(I)$$

where I denotes the input image, and the resulting representation $h_I \in \mathbb{R}^{d_I}$ corresponds to its feature vector, with d_I indicating the dimensionality.

3.1.3 Forgery Feature Extraction

To further enhance the model's ability to recognize forgery content in images, this paper designs a forgery-feature extraction module based on Fourier transformation. This module extracts discriminative forgery features through frequency-domain transformation, multi-scale convolutional sampling, and global-dependency modeling.

Given a color image X of size $H \times W$, for each color channel, its two-dimensional discrete Fourier transform produces a complex spectrum X_{comp} . At the point (u, v) , the computation is defined as:

$$X_{\text{comp}}(u, v) = \sum_{m=0}^{H-1} \sum_{n=0}^{W-1} X(m, n) \cdot e^{-j2\pi(\frac{um+vn}{H+W})}$$

where $X(m, n)$ is the pixel value at coordinate (m, n) in the spatial domain. $X_{\text{comp}}(u, v)$ is the complex value in the frequency domain at coordinate (u, v) , representing the component of the wave with frequency u and v in the original image. According to Euler's formula $e^{j\theta} = \cos \theta + j \sin \theta$ ($j^2 = -1$), pixel values can be decomposed into a combination of sine and cosine waves.

A complex number contains a real part and an imaginary part, which cannot be directly processed by convolutional layers. Therefore, the amplitude spectrum $M(u, v)$ is calculated, representing the energy magnitude of each frequency component:

$$M(u, v) = |X_{\text{comp}}(u, v)| = \sqrt{\text{Re}(X_{\text{comp}}(u, v))^2 + \text{Im}(X_{\text{comp}}(u, v))^2}$$

where Re and Im denote the real and imaginary parts of the complex number, respectively. Since the values of $M(u, v)$ vary widely, directly inputting them into a neural network may cause gradient instability. Therefore, compression is applied:

$$X_{\text{feat}}(u, v) = \ln(1 + M(u, v))$$

To suppress random noise and retain only the mid- and high-frequency components, we define the low-frequency region Ω_{low} as a circular area at the center of the frequency spectrum, with the corresponding indicator function defined as:

$$I_{\Omega}(u, v) = \begin{cases} 1, & \sqrt{(u - H/2)^2 + (v - W/2)^2} \leq R_{\text{low}} \\ 0, & \text{otherwise} \end{cases}$$

The low-frequency truncated feature map is then obtained by:

$$X_{\text{freq}}(u, v) = X_{\text{feat}}(u, v) \cdot (1 - I_{\Omega}(u, v))$$

Finally, the frequency-domain features of the three color channels are stacked to form

$$X_{\text{freq}} \in \mathbb{R}^{H \times W \times 3}.$$

Then, X_{freq} is input to a backbone network, and low-level features are extracted through convolutional layers:

$$F_{\text{backbone}} = \text{CNN}(X_{\text{freq}})$$

where CNN denotes a convolutional neural network, and the output F_{backbone} represents the initial image features.

Next, multi-scale features are obtained using different convolution kernels ($1 \times 1, 3 \times 3, 5 \times 5$) and pooling operations, and the outputs are concatenated:

$$F_{\text{ms}} = [F_{\text{branch1}}, F_{\text{branch3}}, F_{\text{branch5}}, F_{\text{branch_pool}}]$$

To model long-range frequency dependencies across different image regions, the module introduces a multi-head self-attention mechanism. F_{ms} is reshaped and transposed into a sequence $Z \in \mathbb{R}^{L \times C}$, where $L = H' \times W'$, C is the number of feature channels, and $H' \times W'$ is the height and width of the feature map.

For the i -th attention head, the computation is:

$$\text{Attention}(Q_i, K_i, V_i) = \text{softmax}\left(\frac{Q_i K_i^T}{\sqrt{d_k}}\right) V_i$$

where Q, K, V are the queries, keys, and values obtained from Z via linear projection, and $\sqrt{d_k}$ is a scaling factor used to prevent large dot products from causing gradient vanishing.

By concatenating the outputs of N heads and applying a linear projection, an enhanced feature sequence is obtained. Finally, global average pooling (GAP) followed by a fully connected (FC) layer generates the final forgery feature vector:

$$h_{\text{forgery}} = \text{FC}(\text{GAP}(\text{MultiHead}(Z)))$$

3.2 Evidence Fusion Module

To enhance semantic consistency across modalities through contrastive learning between text and evidence, as well as image and evidence, this paper introduces a multi-head attention-based evidence fusion module, inspired by the work of Huang et al. [27].

For textual evidence, we weight the evidence using a multi-head attention mechanism, allowing the selection of relevant evidence based on the main text features. Specifically, given the main text feature h_T as the query, and the textual evidence \tilde{E}_t as keys and values, multi-head attention is computed as follows. First, the main text feature h_T is mapped to a query vector, and the textual evidence features \tilde{E}_t , obtained from BERT, are mapped to key and value vectors:

$$Q = h_T W^Q, K = \tilde{E}_t W^K, V = \tilde{E}_t W^V$$

where W^Q, W^K, W^V are learnable weight matrices.

To capture the relevance between the main text and evidence, the output of the i -th attention head head_i is calculated as:

$$\text{head}_i = \text{Attention}(Q_i, K_i, V_i) = \text{softmax}\left(\frac{Q_i K_i^T}{d_k}\right) V_i$$

All head outputs are then concatenated and passed through a linear transformation to obtain the final attention-weighted evidence feature H_a . The fused textual feature is denoted as H'_T :

$$H'_T = \text{MultiHeadAttn}(Q = h_T, K = \tilde{E}_t, V = \tilde{E}_t)$$

The processing of image evidence is similar to textual evidence. The image feature h_I is used as the query, and the image evidence \tilde{E}_i , obtained by ResNet34, is used as keys and values:

$$H'_I = \text{MultiHeadAttn}(Q = h_I, K = \tilde{E}_i, V = \tilde{E}_i)$$

By integrating external evidence, the model can effectively align across multiple modalities and evidence, ensuring that it focuses on relevant evidence when processing multimodal

information, thereby improving the accuracy of rumor detection.

3.3 Dual contrastive learning module

To strengthen the model's capacity for detecting rumors that exhibit semantic inconsistencies between images and text, this paper designs a dual-contrast similarity perception mechanism. This mechanism consists of two complementary contrastive learning objectives: semantic alignment between text and image descriptions, and semantic alignment between text and visual image features. These two types of alignment constrain the consistency of the feature space at the semantic and visual levels, respectively, thereby improving the model's comprehensive perception of text-image relationships. In particular, it can effectively detect rumors when there is surface-level mismatch between image descriptions and text.

3.3.1 Image Description Generation and Semantic Mapping

Unlike traditional methods that directly compute similarity in the visual feature space, This study employs the BLIP [28] model to produce descriptive captions for images, thereby transforming visual inputs into interpretable textual semantic representations. Similar methods have also been used in [27] and achieved notable results.

Let the original image be I . After processing with the BLIP model, the corresponding textual description is $BLIP(I)$. The semantic feature e_t is then extracted using BERT, as follows:

$$e_t = \text{BERT}(\text{BLIP}(I))$$

3.3.2 Text-Image Description Semantic Alignment

We first compute the semantic similarity between the original text feature h_T and the BLIP-generated image description feature e_t .

Define normalized features u and v . In a batch of size N , the similarity matrix between all texts and all image descriptions is M_{tt} , where the element in the i -th row and j -th column, $s_{i,j}$, represents the similarity between the i -th text and the j -th image description:

$$s_{i,j} = u_i \cdot v_j^T$$

To train the model to recognize consistency, the similarity of positive pairs on the diagonal should be maximized while the similarity of negative pairs off the diagonal should be minimized.

For the i -th sample, the InfoNCE loss is defined as:

$$L_{TT} = -\log \frac{\exp(s_{i,i}/\tau)}{\sum_{j=1}^N \exp(s_{i,j}/\tau)}$$

where $s_{i,i}$ is the score of the positive pair between the current text and its corresponding image description, $s_{i,j}(i \neq j)$ are negative pair scores, and τ is the temperature parameter used to adjust sensitivity to hard negatives.

This loss reinforces the consistency between image content and text descriptions at the semantic level by maximizing the similarity of matching samples ($i = j$) and minimizing the similarity of non-matching samples ($i \neq j$). It effectively detects semantic-level contradictions, for example, when the event described in text does not match the visual scene in the image.

3.3.3 Text-Image Visual Alignment

To ensure semantic coherence at the visual level, the InfoNCE loss for the i -th sample is defined as:

$$L_{TI} = -\log \frac{\exp(s_{i,i}^i/\tau)}{\sum_{j=1}^N \exp(s_{i,j}^i/\tau)}$$

$$s_{i,j}^i = u_i \cdot g_j^T$$

where $s_{i,j}^i$ represents the similarity between the i -th text and the j -th image, and u and g denote the normalized text and image features, respectively.

3.3.4 Joint Optimization of Dual Contrast

The overall objective of the similarity perception module is:

$$\mathcal{L}_{\text{sim}} = \lambda_{TT}L_{TT} + \lambda_{TI}L_{TI}$$

where λ_{TT} and λ_{TI} are balancing coefficients for semantic alignment and visual alignment, respectively.

Through dual-contrast constraints, the model simultaneously learns semantic-level alignment, ensuring consistency between textual descriptions and image content, and visual-level alignment, strengthening the correspondence between text and images in appearance and entities. This semantic–visual dual constraint allows the model to capture subtle cross-modal inconsistencies when encountering mismatched images and text or misleading headlines, thereby significantly improving detection accuracy.

3.4 Gated Modulation Module

In multimodal rumor detection tasks, text and images often exhibit high complexity and uncertainty at the semantic level. Due to the heterogeneous information sources and substantial differences in semantic expression, directly performing feature concatenation or weighted fusion may easily cause semantic conflicts and feature redundancy. Traditional fusion methods usually employ static weighting or simple concatenation, which cannot adaptively adjust the fusion ratio between modalities according to contextual semantic relationships, resulting in inflexible and non-selective feature representation. Different modal features may differ significantly in numerical scale and activation intensity, and directly using them for classification may lead to feature amplification or unstable training.

To address this, an adaptive feature-scaling mechanism is introduced to constrain the overall scale of fused features. Based on this, the paper proposes a gated modulation module that combines the gating mechanism with adaptive feature scaling for fine-grained feature fusion modeling and coarse-grained feature magnitude modulation.

3.4.1 Gated Modulation Mechanism

During the fusion stage, the model applies hierarchical gating control to text and image features to determine the contribution ratio of the main post information and external evidence. Specifically, let the main post text feature be $h_T, h_T \in \mathbb{R}^{d_T}$, and the text feature enhanced by evidence attention be $\tilde{h}_T, \tilde{h}_T \in \mathbb{R}^{d_T}$. Let the main post image feature be $h_I, h_I \in \mathbb{R}^{d_I}$, and the image feature enhanced by evidence attention be $\tilde{h}_I, \tilde{h}_I \in \mathbb{R}^{d_I}$.

The model first concatenates the two features and applies a linear transformation followed by a Sigmoid activation to obtain the inter-modal gating weights:

$$\alpha_T = \sigma(W_T[h_T; \tilde{h}_T]), \quad \alpha_I = \sigma(W_I[h_I; \tilde{h}_I])$$

where $\sigma(\cdot)$ denotes the Sigmoid function, and W_T, W_I are learnable parameter matrices.

Then, the model performs weighted fusion of the main post and evidence features according to the gating coefficients:

$$h_T^{\text{fusion}} = \alpha_T \cdot h_T + (1 - \alpha_T) \cdot \tilde{h}_T, \quad h_I^{\text{fusion}} = \alpha_I \cdot h_I + (1 - \alpha_I) \cdot \tilde{h}_I$$

The gating weights α_T and α_I reflect the importance of different modal features. When the main post information is sufficient, the gating factor tends to increase, allowing the model to retain more of the original semantics. When the external evidence contains strongly relevant

or contradictory information, the gating coefficients decrease, enabling the model to actively incorporate external information for semantic correction.

3.4.2 Cross-Modal Gated Fusion

After completing the single-modal gating, the model further fuses text and image semantic features in the cross-modal space. The gated text feature h_T^{fusion} and image feature h_I^{fusion} are mapped into the same latent space:

$$h'_T = W_C h_T^{\text{fusion}}, \quad h'_I = W_I h_I^{\text{fusion}}$$

Then, a second-layer gating structure implements interaction fusion between the two modalities:

$$\beta = \sigma(W_{TI}[h'_T; h'_I]), \quad h_{TI}^{\text{fusion}} = \beta \cdot h'_T + (1 - \beta) \cdot h'_I$$

where β denotes the cross-modal gating weight, controlling the proportion of text and image in the fused features.

Finally, forgery features are integrated to enhance the model's ability to recognize image manipulation:

$$h_{\text{forgery}} = W_S h_{\text{forgery}}, \quad h_{\text{final}} = \gamma \cdot h_{TI}^{\text{fusion}} + (1 - \gamma) \cdot h_{\text{forgery}}$$

Where $\gamma = \sigma(W_h[h_{TI}^{\text{fusion}}; h_{\text{forgery}}])$, $h_{\text{forgery}} \in \mathbb{R}^f$, $h_{\text{final}} \in \mathbb{R}^f$.

3.4.3 Adaptive Feature Scaling Mechanism

After obtaining the fused features, the model introduces an adaptive feature scaling mechanism to further improve robustness. This mechanism modulates the fused features through a learnable scaling parameter λ :

$$h_{\text{final}} = \lambda \cdot h_{\text{final}}, \quad \lambda \in (0,1]$$

This gating parameter is jointly optimized with the other model parameters during training and is used to adaptively control the overall strength of the fused features. As a result, it mitigates noise interference caused by the accumulation of multimodal features and enhances the stability and generalization ability of the model during training.

3.5 Classifier Design

This study constructs a classification prediction module based on a two-layer perceptron, aiming to perform final category discrimination on the multimodal comprehensive feature h_{final} obtained after gated fusion and adaptive feature scaling. This feature vector deeply integrates and enhances text semantics, image content, and forgery features, providing solid evidence for authenticity determination.

In implementation, the classifier first maps the fused features to a high-dimensional space through the first fully connected layer FC_1 , embedding a LeakyReLU activation function to alleviate the “dead neuron” problem in deep networks and ensure continuous effective gradient flow during model iterations. The second fully connected layer FC_2 then maps the feature to a category prediction space of dimension \mathcal{C} , outputting unnormalized logit vector h_{class} . Finally, the model applies the Softmax function to convert this vector into a predicted probability distribution y .

$$h_{\text{class}} = \text{FC}_2(\text{LeakyReLU}(\text{FC}_1(h_{\text{final}}))), \quad y = \text{Softmax}(h_{\text{class}})$$

where y denotes the output probability distribution of the classifier.

The classifier is trained using the cross-entropy loss, which is commonly employed in classification tasks. The cross-entropy loss measures the difference between the predicted distribution and the ground-truth label distribution. For single-sample classification, the loss is defined as:

$$\mathcal{L}_{\text{class}} = - \sum_{i=1}^C p_i \log(q_i)$$

where C is the number of classes, p_i is the ground-truth probability for class i , and q_i is the predicted probability for class i .

4. Experiments

This section outlines the experimental protocol used to assess the proposed method. The WR2 datasets are introduced first, followed by implementation settings and evaluation metrics. Results are then reported for hyperparameter sensitivity, state-of-the-art comparisons, ablations, and error analysis. A final case study illustrates practical strengths and remaining limitations.

4.1 Datasets

This study uses the MR2 dataset, released by Hu et al. [29], which is specifically designed for multimodal rumor detection. MR2 consists of two sub-datasets from Twitter and Weibo, covering content from English and Chinese social media platforms. Each sample contains a text paragraph and an accompanying image. The samples are labeled into three categories: rumor, non-rumor, and unconfirmed rumor.

The construction of the MR2 dataset not only involves collecting text-image pairs but also retrieving additional textual and visual evidence from the web. Image evidence is typically obtained through reverse image search of the original image, while textual evidence is acquired by searching the original text to collect relevant web page titles, summaries, and other textual information.

4.2 Experimental Settings and Evaluation Metrics

In this experiment, the dataset is split into training, validation, and test sets with a ratio of 8:1:1. The maximum text length is set to 40 tokens to accommodate most Twitter and Weibo samples. In practice, the maximum number of text and visual evidence items for each post is set to 5, and 8 attention heads are used for cross-attention.

The classification task employs a two-layer perceptron network. During training, the model uses the AdamW optimizer with an initial learning rate of 5×10^{-5} , a batch size of 32, and a total of 8 training epochs. Learning rate adjustment is performed using the ExponentialLR scheduler to dynamically tune the learning rate and improve training efficiency.

To prevent overfitting, an early stopping strategy with a patience of 2 is employed, meaning training stops when validation performance no longer improves. The method is implemented based on the PyTorch deep learning framework. Macro Accuracy (M_ACC), Precision (PRE), Recall (REC), and F1-score (F1) are adopted as the main evaluation metrics to comprehensively assess the model's performance in rumor detection tasks.

4.3 Experimental Results and Analysis

4.3.1 Effect of Evidence Quantity

The maximum number of retrieved evidence items is a critical hyperparameter: too little evidence limits context for verification, whereas too much increases the risk of irrelevant or incorrect matches. Figure 2 reports a sweep of retrieved text/visual evidence from 1 to 9 items and the corresponding macro accuracy on Weibo and Twitter. Performance peaks at 5 evidence items on both datasets, indicating that evidence quantity and quality jointly shape verification: under-retrieval leaves claims under-supported, while over-retrieval injects noise

that degrades classification.

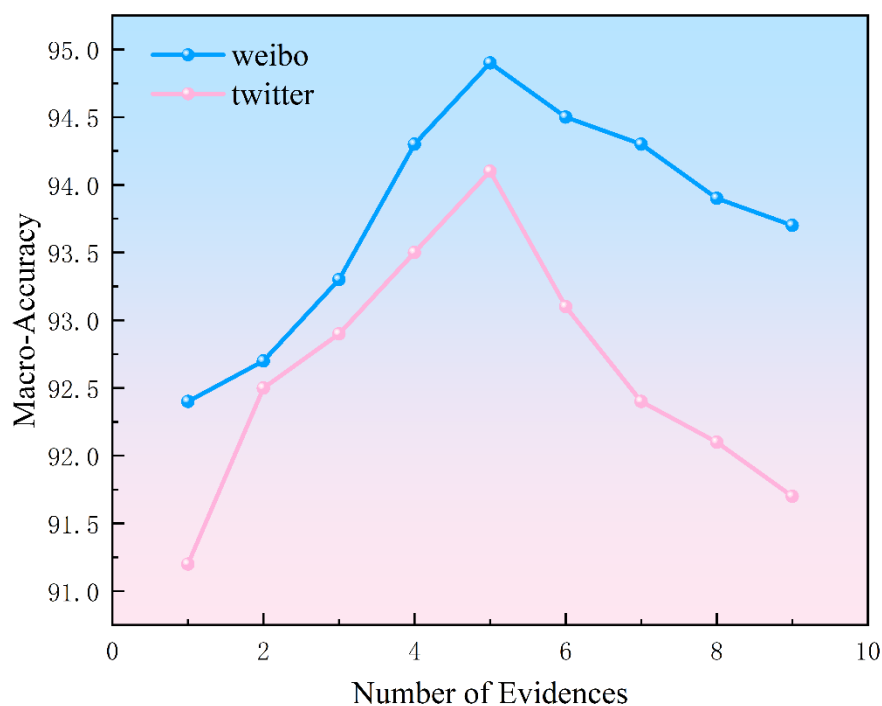


Figure 2. The impact of evidence quantity

4.3.2 Comparison with Baseline Methods

To verify the effectiveness of our proposed method, we selected the following six methods as comparison baselines:

CLIP [30]: Uses the image encoder of CLIP to extract image features, and classifies the feature vector corresponding to the special token “CLS” via a linear layer.

LSTM_word2vec [9]: A text-only detection method. It employs word2vec and LSTM to extract semantic features from text content for rumor detection.

DEDA [10]: A text-only detection method. It utilizes a deep normalized attention mechanism to extract sentiment features from text for rumor judgment.

HMCAN [31]: A multimodal detection method. It employs a hierarchical multimodal context attention network (HMCAN) to model contextual information in both text and images for rumor detection.

CCN [23]: A multimodal detection method specifically designed to address the selective distortion problem in text–image mismatches. It uses a Consistency Checking Network (CCN) to learn and determine whether external evidence is consistent with post content.

MRAN [32]: A multimodal method that detects fake news through an attention network modeling both intramodal and intermodal relationships.

To verify the effectiveness of the method, this paper compares six rumor detection methods on two datasets of different languages, Weibo and Twitter. 错误!未找到引用源。 and 错误!未找到引用源。 show that the method in this paper achieves the best results in both cases. It reaches a Macro-F1 of 94.9% on the Weibo dataset and 94.1% on the Twitter dataset. These results verify the effectiveness of the multimodal fusion strategy proposed in this paper and demonstrate its leading performance in cross-linguistic scenarios, indicating that the method possesses good language-independent characteristics.

The results show that, due to ignoring information in either text or graphic features, rumor detection methods relying on a single modality are generally inferior to multimodal rumor detection methods. Multimodal rumor detection methods can distinguish rumors through more information; therefore, the macro accuracy of multimodal models is significantly improved. Among many multimodal baseline models, this method is slightly superior to CCN, which introduces external evidence, and MRAN, which introduces a cross-attention mechanism; the advantage lies in the addition of image forgery feature enhancement, demonstrating the importance of forged image identification for rumor detection.

Table 1: The comparative experiment on the Weibo dataset.

	Non-rumor				Rumor			Unverified		
	Macro Accuracy	Precision	Recall	F1 Score	Precision	Recall	F1 Score	Precision	Recall	F1 Score
CLIP	82.8	88.7	90.3	89.5	87.2	75.6	81.0	78.2	82.5	80.3
LSTM_Word2vec	86.3	90.5	91.6	91.1	82.8	78.1	80.4	87.5	89.3	88.4
DEDA	88.6	93.6	93.4	93.5	84.6	81.5	83.0	89.1	90.9	90.0
HMCAN	89.7	95.9	94.2	95.0	86.1	82.6	84.3	89.4	92.3	90.8
CCN	92.0	96.7	95.5	96.1	85.7	87.9	86.8	93.9	93.5	93.7
MRAN	92.7	97.1	94.4	95.7	84.4	91.2	87.7	94.5	92.4	93.4
ours	94.9	95.1	96.3	95.7	88.6	96.1	92.2	97.3	92.3	94.7

Table 2: The comparative experiment on the Twitter dataset.

	Non-rumor				Rumor			Unverified		
	Macro Accuracy	Precision	Recall	F1 Score	Precision	Recall	F1 Score	Precision	Recall	F1 Score
CLIP	83.8	92.6	85.3	88.8	81.3	79.8	80.5	81.1	86.3	83.6
LSTM_Word2vec	87.0	89.6	91.8	90.7	82.4	76.8	79.5	91.2	92.4	91.8
DEDA	88.8	91.9	93.4	92.6	84.9	79.5	82.1	91.8	93.4	92.6
HMCAN	89.9	92.9	93.7	93.3	85.4	82.2	83.8	92.8	93.8	93.3
CCN	91.8	94.8	95.7	95.2	88.7	84.5	86.5	93.8	95.2	94.5
MRAN	92.5	93.3	97.1	95.2	93.3	86.0	89.5	93.7	94.3	94.0

ours 94.1 97.9 95.5 96.7 85.5 91.5 88.4 96.8 95.4 96.1

4.3.3 Ablation Study

To verify the contribution of each module, we design the following seven ablation experiments:

1. w/o D C: The Dual contrastive learning module is removed.
2. w/o Forgery: The forgery feature extraction module is removed.
3. w/o Gating: The gated fusion and adaptive feature scaling mechanisms are removed.
4. w/o Evidence: Both textual and visual evidence are removed.
5. w/o T-I D C: The text-image contrastive learning module is removed.
6. w/o T-T D C: The text-image description contrast module is removed.
7. w/o F S: Only the adaptive feature scaling mechanism is removed.

The results on the Weibo and Twitter datasets are shown in Tables 3 and 4, respectively. By comparing the full model with these seven variants, the ablation study effectively validates the necessity and effectiveness of each component in the model.

Table 1 . The ablation experiment results on the Weibo dataset

	Non-rumor			Rumor			Unverified			
	Accuracy	Precision	Recall	F1 Score	Precision	Recall	F1 Score	Precision	Recall	F1 Score
w/o DC	93.1	96.7	97.1	96.9	92.8	87.1	89.9	92.5	95.1	93.8
w/o Forgery	92.2	96.7	97.9	97.3	87.9	85.9	86.9	92.6	92.9	92.8
w/o Gating	91.4	95.1	95.5	95.3	90.9	83.7	87.2	91.7	95.1	93.4
w/o Evidence	91.9	98.3	92.9	95.5	88.5	86.5	87.5	91.8	96.3	94.0
w/o T-I DC	93.7	96.7	96.3	96.5	89.4	90.4	89.9	94.6	94.3	94.4
w/o T-T DC	94.1	98.3	94.2	96.2	91.1	92.1	91.6	93.8	96.0	94.9
w/o FS	93.5	97.1	95.9	96.5	90.0	89.3	89.6	94.2	95.4	94.8
ours	94.9	95.1	96.3	95.7	88.6	96.1	92.2	97.3	92.3	94.7

Table 2. The ablation experiment results on the Twitter dataset

	Non-rumor			Rumor			Unverified			
	Accuracy	Precision	Recall	F1 Score	Precision	Recall	F1 Score	Precision	Recall	F1 Score
w/o DC	92.4	93.8	98.5	96.1	87.2	84.5	85.8	96.4	94.3	95.3
w/o Forgery	91.1	92.9	98.5	95.6	93.5	77.5	84.8	93.9	97.2	95.5
w/o Gating	91.7	95.5	95.5	95.5	82.7	85.3	84.0	95.7	94.3	95.0
w/o Evidence	91.8	96.4	94.0	95.2	80.7	87.6	84.0	96.0	93.9	94.9
w/o T-I DC	93.0	95.6	98.0	96.8	82.7	89.1	85.8	97.0	91.8	94.3
w/o T-T DC	93.2	95.6	97.5	96.5	92.4	84.5	88.3	95.1	97.5	96.3
w/o FS	92.9	97.0	98.0	97.5	93.0	82.9	87.7	93.9	97.9	95.9
ours	94.1	97.9	95.5	96.7	85.5	91.5	88.4	96.8	95.4	96.1

The experimental results in Table 1 and Table 2 show that the complete model achieves

optimal performance on most evaluation metrics. This indicates that each module realizes effective collaborative effects. Among all ablation settings, removing the gating module and the image forgery feature extraction module causes the most significant performance degradation. Specifically, after removing the gating mechanism, the macro accuracy on the Weibo dataset drops by 3.5%. The impact on the F1 Score of the rumor category is significant. This proves that the gating mechanism plays an important role in regulating information flow and filtering noise. After removing the image forgery feature extraction, the macro accuracy on the Twitter dataset decreases by 3.0%. This indicates that capturing image tampering traces is crucial for rumor detection, especially on image-rich platforms like Twitter. The absence of the dual contrastive learning module also leads to a significant drop in macro accuracy compared to removing a single contrastive component. This validates the effectiveness of jointly optimizing intra-modal and inter-modal semantic consistency. Removing the evidence fusion module similarly causes substantial performance decline. This highlights the auxiliary role of evidence information in rumor judgment. Although the performance loss after removing the adaptive feature scaling mechanism is relatively small, it still causes stable performance degradation. This demonstrates that these components contribute positively to the model's robustness and dynamic adaptability. In summary, the proposed model achieves efficient and robust detection of multimodal rumors through the integration of the above key mechanisms.

4.3.4 t-SNE Feature Visualization Analysis

To evaluate the model's discriminative efficacy during multimodal fusion, Figure 3 presents t-SNE visualizations of fused features across the Weibo and Twitter datasets, Blue, brown and cyan represent non-rumor, rumor and unverified samples respectively. The resulting low-dimensional distribution exhibits strong inter-class distinguishability. This is evidenced by the formation of distinct clusters for different samples. The minimal overlap in transition regions indicates that the model retains flexible representations for semantically ambiguous or conflicting samples. This avoids imposing strict boundaries. The continuity of this structure is largely facilitated by the adaptive feature scaling mechanism. This mechanism produces a smoother and more resilient fused feature space.

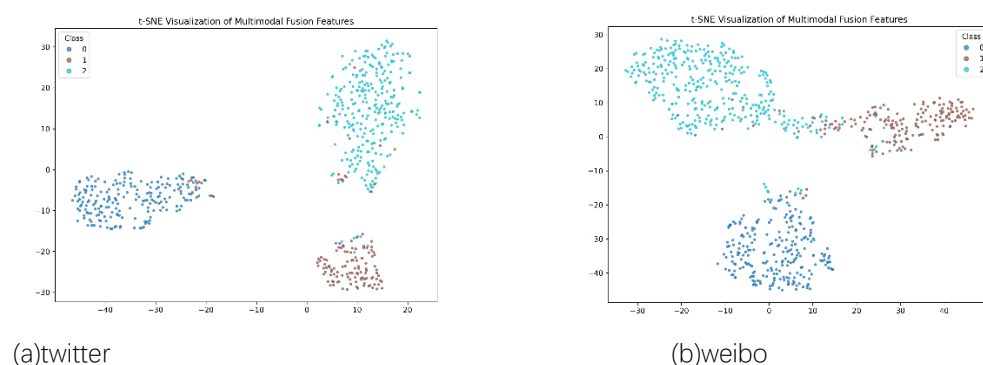


Figure 3. t-SNE Feature Visualization

4.3.5 Error Analysis

To conduct a detailed analysis of prediction errors, we visualized the confusion matrices of the test results, as shown in Figure 4. The horizontal axis and vertical axis represent predictions and ground truth labels respectively. Despite achieving superior macro accuracy on Weibo and Twitter datasets, the detailed category-specific performance highlights inherent

challenges in handling diverse information types. Although the model F1 score exceeds 94% in non-rumor and unverified categories, the rumor performance on Twitter drops to 88.4%, while on Weibo it is 92.2%. This highlights the difficulty of identifying stealthy misinformation on Twitter. The precision and recall on the Weibo dataset show that the model tends to identify information as rumors. The unverified category exhibits high precision and relatively low recall. This indicates that the model is very cautious when confirming information in this class.

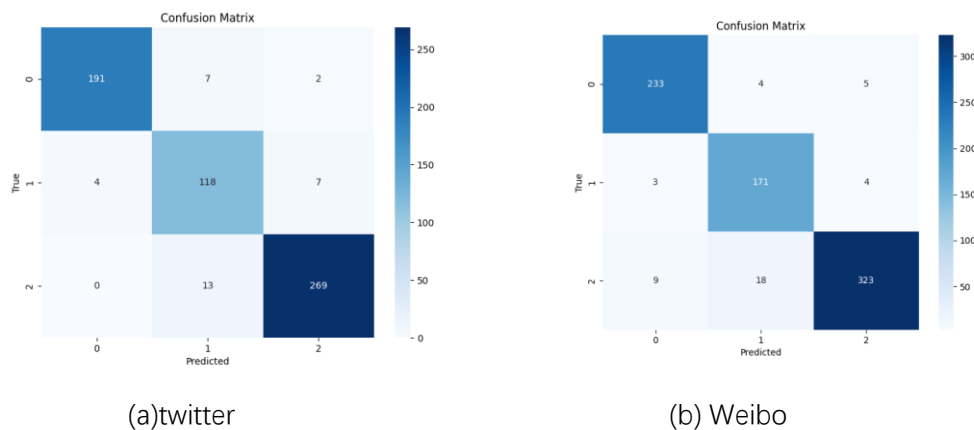


Figure 4. Confusion matrix visualization

5. Conclusion

This paper proposes a rumor detection method based on the enhancement of external evidence and forgery features, and significantly improves the model's performance in rumor detection tasks by introducing a dual contrastive learning mechanism and a gated modulation module. Experiments on the MR2 dataset show improvements in multimodal reasoning, image forgery sensitivity, and cross-modal semantic alignment. The research results indicate that a balance exists between evidence and noise: insufficient evidence lacks context, while excessive evidence hinders the integration of relevant content; therefore, the quantity of evidence must be selected. By introducing a feature fusion method with an adaptive mechanism, the model can automatically adjust fusion weights based on the importance of features, effectively reducing the negative impact of noise on performance. Future work will explore more fine-grained integration methods and extend evidence collection strategies in high-noise and complex scenarios.

6. References

1. Tufchi S, Yadav A, Ahmed T. A comprehensive survey of multimodal fake news detection techniques: Advances, challenges, and opportunities. *Int J Multimed Inf Retr.* 2023;12(2):28. <https://doi.org/10.1007/s13735-023-00296-3>
2. Guo X, Liu X, Ren Z, Grosz S, Masi I, Liu X. Hierarchical fine-grained image forgery detection and localization. In: *Proceedings of the IEEE/CVF Conference on Computer Vision and Pattern Recognition*; 2023. p. 3155–3165. <https://doi.org/10.1109/CVPR52729.2023.00308>
3. Wang B, Wu X, Tang Y, Ma Y, Shan Z, Wei F. Frequency domain filtered residual network for deepfake detection. *Mathematics.* 2023;11(4):816. <https://doi.org/10.3390/math11040816>
4. Wang L, Zhang C, Xu H, Xu Y, Xu X, Wang S. Cross-modal contrastive learning for multimodal fake news detection. In: *Proceedings of the 31st ACM International Conference on Multimedia*; 2023 Oct. p. 5696–5704. <https://doi.org/10.1145/3581783.3613850>

5. Li J, Bin Y, Zou J, Wei J, Wang G, Yang Y. Cross-modal consistency learning with fine-grained fusion network for multimodal fake news detection. In: Proceedings of the 5th ACM International Conference on Multimedia in Asia; 2023 Dec. p. 1–7. <https://doi.org/10.1145/3595916.3626397>
6. Kwon S, Cha M, Jung K, Chen W, Wang Y. Prominent features of rumor propagation in online social media. In: Proceedings of the 2013 IEEE 13th International Conference on Data Mining; 2013 Dec. p. 1103–1108. <https://doi.org/10.1109/ICDM.2013.61>
7. Ma J, Gao W, Mitra P, Kwon S, Jansen BJ, Wong KF, et al. Detecting rumors from microblogs with recurrent neural networks. In: Proceedings of the 25th International Joint Conference on Artificial Intelligence; 2016. p. 3818–3824.
8. Chen T, Li X, Yin H, Zhang J. Call attention to rumors: Deep attention based recurrent neural networks for early rumor detection. In: Pacific-Asia Conference on Knowledge Discovery and Data Mining; 2018. p. 40–52. https://doi.org/10.1007/978-3-030-04503-6_4
9. Alkhodair SA, Ding SH, Fung BC, Liu J. Detecting breaking news rumors of emerging topics in social media. *Inf Process Manag.* 2020;57(2):102018. <https://doi.org/10.1016/j.ipm.2019.02.016>
10. Luvembe AM, Li W, Li S, Liu F, Xu G. Dual emotion based fake news detection: A deep attention-weight update approach. *Inf Process Manag.* 2023;60(4):103354. <https://doi.org/10.1016/j.ipm.2023.103354>
11. Xu F, Sheng VS, Wang M. Near real-time topic-driven rumor detection in source microblogs. *Knowl Based Syst.* 2020;207:106391. <https://doi.org/10.1016/j.knosys.2020.106391>
12. Cao J, Qi P, Sheng Q, Yang T, Guo J, Li J. Exploring the role of visual content in fake news detection. In: *Disinformation, Misinformation, and Fake News in Social Media: Emerging Research Challenges and Opportunities.* 2020. p. 141–161. https://doi.org/10.1007/978-3-030-42699-6_8
13. Qi P, Cao J, Yang T, Guo J, Li J. Exploiting multi-domain visual information for fake news detection. In: Proceedings of the 2019 IEEE International Conference on Data Mining; 2019 Nov. p. 518–527. <https://doi.org/10.1109/ICDM.2019.00062>
14. Huang Y, Sun L. FakeGPT: Fake news generation, explanation and detection of large language models. *arXiv.* 2023;arXiv:2310.05046. <https://doi.org/10.48550/arXiv.2310.05046>
15. Zhang X, Gao W. Towards LLM-based fact verification on news claims with a hierarchical step-by-step prompting method. In: Proceedings of the 13th International Joint Conference on Natural Language Processing and the 3rd Conference of the Asia-Pacific Chapter of the Association for Computational Linguistics; 2023 Nov. p. 996–1011. <https://doi.org/10.48550/arXiv.2310.00305>
16. Wang Y, Ma F, Jin Z, Yuan Y, Xun G, Jha K, et al. EANN: Event adversarial neural networks for multi-modal fake news detection. In: Proceedings of the 24th ACM SIGKDD International Conference on Knowledge Discovery & Data Mining; 2018 Jul. p. 849–857. <https://doi.org/10.1145/3219819.3219903>
17. Nguyen DM, Do TH, Calderbank R, Deligiannis N. Fake news detection using deep Markov random fields. In: Proceedings of the 2019 Conference of the North American Chapter of the Association for Computational Linguistics; 2019 Jun. p. 1391–1400. <https://doi.org/10.18653/v1/n19-1142>
18. Kirchknopf A, Slijepčević D, Zeppelzauer M. Multimodal detection of information disorder from social media. In: Proceedings of the International Conference on Content-Based Multimedia Indexing; 2021 Jun. p. 1–4. <https://doi.org/10.1109/CBIMI50390.2021.9485012>
19. Luvembe AM, Li W, Li S, Liu F, Wu X. CAF-ODNN: Complementary attention fusion with optimized deep neural network for multimodal fake news detection. *Inf Process Manag.* 2024;61(3):103653. <https://doi.org/10.1016/j.ipm.2024.103653>

20. Liu X, Pang M, Li Q, Zhou J, Wang H, Yang D. MVACNet: A multimodal virtual augmentation contrastive learning network for rumor detection. *Algorithms*. 2024;17(5):199. <https://doi.org/10.3390/a17050199>
21. Zhou X, Wu J, Zafarani R. Similarity-aware multi-modal fake news detection. In: *Pacific-Asia Conference on Knowledge Discovery and Data Mining*; 2020. p. 354–367. https://doi.org/10.1007/978-3-030-47436-2_27
22. Xue J, Wang Y, Tian Y, Li Y, Shi L, Wei L. Detecting fake news by exploring the consistency of multimodal data. *Inf Process Manag*. 2021;58(5):102610. <https://doi.org/10.1016/j.ipm.2021.102610>
23. Abdelnabi S, Hasan R, Fritz M. Open-domain, content-based, multi-modal fact-checking of out-of-context images via online resources. In: *Proceedings of the IEEE/CVF Conference on Computer Vision and Pattern Recognition*; 2022. p. 14940–14949.
24. Zhang X, Dadkhah S, Weismann AG, Kanaani MA, Ghorbani AA. Multimodal fake news analysis based on image–text similarity. *IEEE Trans Comput Soc Syst*. 2023;11(1):959–972. <https://doi.org/10.1109/TCSS.2023.3241571>
25. Wu K, Cao D. Evidence-aware multimodal Chinese social media rumor detection. In: *Proceedings of the IEEE International Conference on Acoustics, Speech and Signal Processing*; 2024 Apr. p. 8376–8380. <https://doi.org/10.1109/ICASSP48485.2024.10447346>
26. Wu Y, Sun J, Yuan X, Huang Z, Dai J. Dual-channel early rumor detection based on factual evidence. *Expert Syst Appl*. 2024;238:121928. <https://doi.org/10.1016/j.eswa.2023.121928>
27. Huang X, Ma T, Rong H, Jia L, Su Y. Dual evidence enhancement and text–image similarity awareness for multimodal rumor detection. *Eng Appl Artif Intell*. 2025;153:110845. <https://doi.org/10.1016/j.engappai.2025.110845>
28. Li J, Li D, Xiong C, Hoi S. BLIP: Bootstrapping language-image pre-training for unified vision-language understanding and generation. In: *Proceedings of the International Conference on Machine Learning*; 2022 Jun. p. 12888–12900.
29. Hu X, Guo Z, Chen J, Wen L, Yu PS. MR2: A benchmark for multimodal retrieval-augmented rumor detection in social media. In: *Proceedings of the 46th International ACM SIGIR Conference on Research and Development in Information Retrieval*; 2023 Jul. p. 2901–2912. <https://doi.org/10.1145/3539618.3591896>
30. Radford A, Kim JW, Hallacy C, Ramesh A, Goh G, Agarwal S, et al. Learning transferable visual models from natural language supervision. In: *Proceedings of the International Conference on Machine Learning*; 2021 Jul. p. 8748–8763.
31. Qian S, Wang J, Hu J, Fang Q, Xu C. Hierarchical multi-modal contextual attention network for fake news detection. In: *Proceedings of the 44th International ACM SIGIR Conference on Research and Development in Information Retrieval*; 2021. p. 153–162. <https://doi.org/10.1145/3404835.3462871>
32. Yang H, Zhang J, Zhang L, Cheng X, Hu Z. MRAN: Multimodal relationship-aware attention network for fake news detection. *Comput Stand Interfaces*. 2024;89:103822. <https://doi.org/10.1016/j.csi.2023.103822>